High sensitivity and low detection limit sensor based on a slotted nanobeam cavity in silicon

Mohannad Al-Hmoud,* and Rasha Alyahyan

Physics Department, College of Science, Imam Mohammad ibn Saud Islamic University (IMSIU), P.O. Box 90950, Riyadh 11623, Saudi Arabia

Received June 25, 2022; accepted July 27, 2022; published September 30, 2022

Abstract—In this work, the three-dimensional finite-difference time-domain (3D-FDTD) method is used to design and analyze a refractive index sensor based on a slotted photonic crystal nanobeam cavity. These type of cavity support a high quality-factor and a small volume and therefore is attractive for optical sensing. We demonstrate that when immersing our proposed sensor in water it can possess a high-quality factor of 2.0×10^6, high sensitivity of 325 nm/RIU, and a detection limit of 2.4×10^{-7} RIU. We believe that our proposed sensor is a promising candidate for potential applications in sensing like optofluidic- and bio-sensing.

Among the currently available optical sensors, photonic crystal-based sensors [1,2] are very promising for biosensing due to their small mode volume and high quality-factor (Q). In particular, 1D nanobeam photonic crystal cavities [3,4] can have ultrahigh Q and confine light into ultrasmall volumes. However, the electric field is usually maximized in the dielectric region, which reduces the interaction with the analyte. On the other hand, by introducing an air slot to the cavity region, the obtained structure confines the electric field strongly in the air region [5–7], which results in optimal light-matter interaction. Here, we present a slotted nanobeam cavity as a high-sensitivity refractive index sensor, which can be used in various applications like optofluidic sensing and biosensing.

Optical cavity sensing schemes are based on monitoring shifts of the resonances of high-Q cavities, due to the induced refractive index changes in the near-field of the structure [8]. The sensitivity of a photonic crystal cavity is defined as wavelength shift per refractive index unit [9]: Providing the proper reference to the formula, for instance: https://doi.org/10.1364/OE.460318:

$$S = \frac{\Delta\lambda}{\Delta n}, \qquad (1)$$

where $\Delta\lambda$ is the shift of the resonant wavelength due to the change of the refractive index (Δn) of the environment.

A smaller mode volume V and stronger light confinement in the cavity region can lead to a larger $\Delta\lambda$ and then result in higher sensitivity [10]. Another factor to assess the performance of the sensor is the detection limit (DL). The DL is the minimum RI change that can be measured and is given by [10,11]

$$DL = \frac{\lambda_0}{10QS}, \qquad (2)$$

where λ_0 is the resonant wavelength. Therefore, high sensitivity and high Q are essential for improving the sensing properties of the sensor.

The first step in designing the sensor is the calculation of the photonic band structure (PBS) of an unperturbed 1D nanobeam photonic crystal. The photonic band gap (PBG) should be centered around the desired resonance frequency, which is in our case the telecom wavelength ~ 1550 nm. For this purpose, we used the FDTD method to calculate the PBS. Figure 1 shows the transverse electric (TE) photonic band structure of a 1D nanobeam photonic crystal with the following parameters [5]: Lattice constant $a = 510$ nm, air hole radius $r = 0.365a$, and thickness $t = 220$ nm. The dielectric constant for silicon is set to ε =12.1. The PBG extends from 0.26 to 0.33, which corresponds to 1270 to 1750 nm.

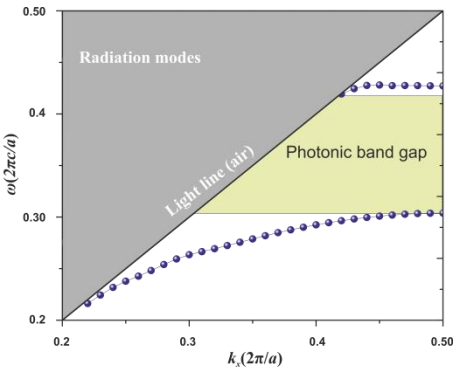

Fig. 1. TE photonic band structure of a 1D nanobeam photonic crystal with lattice constant $\boldsymbol{a}$ = 510 nm, air-hole radius $\boldsymbol{r} = 0.365\boldsymbol{a}$, and thickness $\boldsymbol{t}$ = 220 nm.

The design of optimized geometry of a slotted NPCC is illustrated in Fig. 2(a). The cavity is formed by introducing an air slot to the middle of a rectangular waveguide structure with periodic air holes. Light confinement is achieved by distributed Bragg reflection along the waveguide (x-direction) and by the total internal reflection in the y- and z-directions. For unmodified

* E-mail: mmalhmoud@imamu.edu.sa

structures, the cavity mode terminates abruptly at the mirror boundaries, which leads to large radiation losses and consequently to a low Q (use abbreviation). Fortunately, a proper design of the cavity and its surrounding can improve the Q factor significantly. The optimization mechanism is based on impedance matching between the waveguide mode and the Bloch mode [12–13]. In the design, the photonic crystal mirror, the taper, and the cavity length are engineered to ensure a smooth change in the mode field that penetrates the mirror region. This modification reduces the impedance mismatch between the waveguide mode and the Bloch mode. Therefore, the radiation loss is drastically reduced and a high Q is realized.

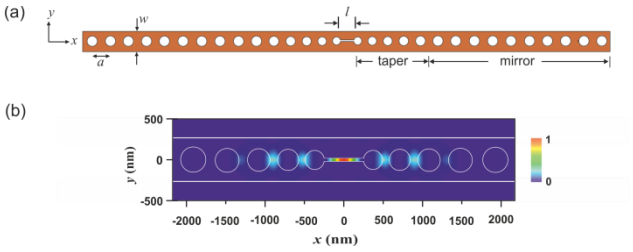

Fig. 2. a) Schematic representation of the optimized slotted nanobeam cavity with $\boldsymbol{a} = 510$ nm, $\boldsymbol{w} = 550$ nm, $\boldsymbol{t} = 220$ nm, and $\boldsymbol{l} = 486$ nm. b) Electric field intensity ($|\boldsymbol{E}|^2$) distribution of the fundamental mode at the plane of $\boldsymbol{z} = 0$. The resonant wavelength in this case is 1581 nm.

When an air slot is introduced at the center of the cavity, the electric field is strongly localized in the air region. This is a consequence of the boundary condition on the normal component of the electric displacement [5,14]. The normal component of the electric displacement (D) across the silicon-air interface is continuous, thus, $\varepsilon_{air}E_{air\perp} = \varepsilon_{si}E_{si\perp}$, where ε_{air} and ε_{si} are the permittivities of air and silicon, respectively. The direction of the electric field is predominantly perpendicular to the silicon-air interface. The electric field intensity distribution of the fundamental mode is shown in Fig. 2(b). It is clear that the electric field intensity is strongly confined in the slot region and therefore can interact with the analyte efficiently. Thus, this type of cavity is a promising device for optical sensing applications.

First, we show the optimization process of the Q factor for a slotted cavity. The periodicity of the air holes in the mirror region is $a = 510$ nm, and the waveguide width (w) and thickness (t) are set to $w = 550$ nm and $t = 220$ nm, respectively. In the simulations, we included 15 air holes pairs on either side of the cavity to increase the photonic mirror strength and reduce the radiation loss.

The five holes closest to the cavity are linearly tapered in both radius and spacing to 67% of their value in the mirror region. In the mirror section, the ratio of the air-hole radius to the periodicity r/a is fixed to 0.36. The refractive index of silicon is set to $n = 3.48$. The slot width is set at 40 nm. The chosen parameters center the photonic bandgap around the telecom wavelength (~1550 nm). With the specified parameters, the cavity supports five quasi-TE modes with resonant wavelengths of 1380, 1554, 1600, 1685, and 1720 nm. Here, we consider only the fundamental mode at 1554 nm due to its better response for Q factor optimization. Moreover, the electric field is highly localized in the slot region, which results in higher interaction with the analyte. The mode volume in this case is $V_{eff} \sim 0.01(\lambda/n)^3$.

The optimization process is based on scanning the cavity length l to find the optimal condition, which ~~that~~ results in matching between the waveguide mode and the Bloch mode. We scan the cavity length over the range from 481 nm to 492 nm. Fig. 3(a) shows the results of the calculation. A maximum Q of 6.6×10^6 is realized for an optimal cavity length of $l = 486$ nm.

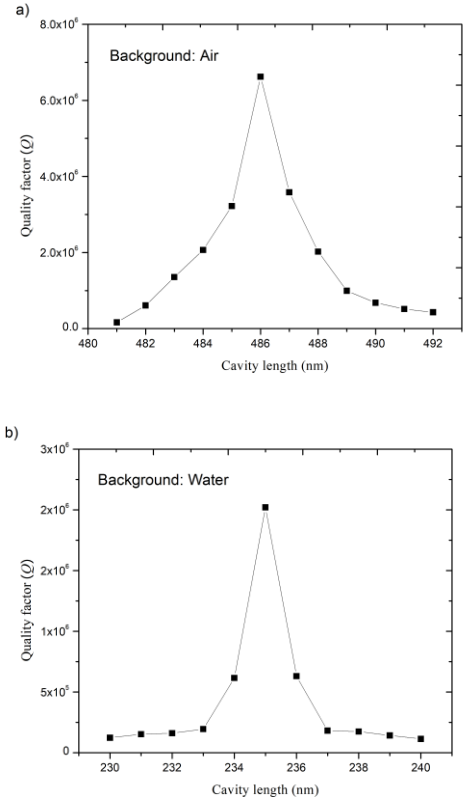

Fig. 3. Q-factor and the resonant wavelength of the fundamental mode as a function of the cavity length l when the background material is (a) air and (b) water.

To investigate the performance of the optimized slotted nanobeam cavity as a refractive index sensor, we test the resonance shift of the fundamental modes due to different salinity concentration of seawater. It is important to note that changing the environment surrounding the sensor from air to sea water will change the optimized parameters for the Q-factor. Also, a redshift in the resonant wavelength is expected. For the water environment (n =1.333) we used the same parameters ($a = 510$ nm,

$w = 550$ nm, and $t = 220$ nm) mentioned earlier for air. In a water environment, the maximum Q of our sensor is 2.0×10^6 at cavity length l =235 nm, as can be seen from Fig. 3(b). A small change in the refractive index results in a shift in the resonant wavelength. To compute the sensitivity of the sensor, we monitored the wavelength shift for different concentrations (0, 10, 20, and 30 g/mole) of seawater salinity. The corresponding RI values for these concentrations are $n = 1.33300, 1.33485, 1.33670$, and 1.33851, respectively [15]. Figure 4(a) shows the wavelength spectra of the fundamental mode of a slotted cavity and the resonant wavelength as a function of the refractive index calculated for different salt concentrations. By increasing RI from 1.33300 to 1.33851, the resonant wavelength shifts from 1568.37 to 1569.33 nm. The sensor exhibits a linear dependence of wavelength shift on the RI. Using Eq. (1) and the results in Fig. 4(b), the calculated sensitivity of the slotted nanobeam sensor is 325 nm/RIU. According to Eq. (2), the detection limit of our device is 2.4×10^{-7}.

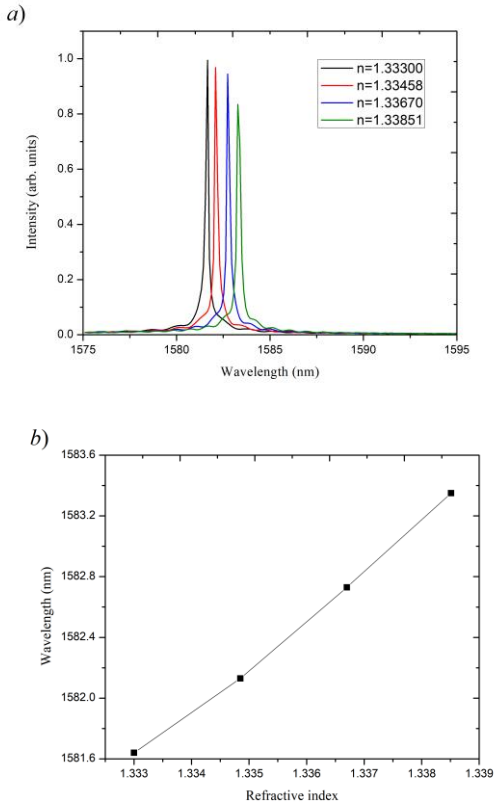

Fig. 4. a) Spectral response of a slotted cavity immersed in seawater with different salinity. Here n=1.333, 1.33485, 1.33670, and 1.33851 correspond to salt concentrations of 0, 10, 20 and 30 g/mole. b) Resonant wavelength as a function of the refractive index.

In conclusion, we presented a slotted nanobeam photonic crystal cavity for refractive index sensing. The performance of the sensor was tested for seawater with different salinity. For an optimized slotted cavity, we demonstrated a high Q-factor of 2.0×10^6, high sensitivity of 325 nm/RIU, and a low detection limit of 2.4×10^{-7} RIU. Owing to the small mode volume, a slotted cavity would allow the detection of single particles. Therefore, this type of cavity is an attractive platform for biosensing or other applications where a small mode volume is required.

The authors extend their appreciation to the Deanship of Scientific Research at Imam Mohammad Ibn Saud Islamic University for funding and supporting this work through Graduate Students Research Support Program.

References

[1] E. Chow, A. Grot, L. Mirkarimi, M. Sigalas, G. Girolami OSA Trends Opt. Photonics Ser. **97**, 909 (2004).
[2] S. Kim, H.-M. Kim, Y.-H. Lee Opt. Lett. **40** 5351 (2015).
[3] D.-Q. Yang, B. Duan, X. Liu, A.-Q. Wang, X.-G. Li, Y.-F. Ji, Micromachines **11**, 72 (2020).
[4] P.B. Deotare, M.W. McCutcheon, I.W. Frank, M. Khan, M. Lončar, Appl. Phys. Lett. **94**, 121106 (2009).
[5] P. Seidler, K. Lister, U. Drechsler, J. Hofrichter, T. Stöferle, Opt. Expr. **21**, 32468 (2013).
[6] H. Choi, M. Heuck, D. Englund, Phys. Rev. Lett. **118**, 223605 (2017).
[7] M. Al.-Hmoud, S. Bougouffa, Results Phys. **26**, 104314 (2021).
[8] M.J. Burek, Y. Chu, M.S. Liddy, P. Patel, J. Rochman, S. Meesala, M. Lončar, Nature Comm. **5**(1), 1 (2014).
[9] M.A. Butt, C. Tyszkiewicz, P. Karasiński, M. Zięba, D. Hlushchenko, T. Baraniecki, A. Kaźmierczak, R. Piramidowicz, M. Guzik, A. Bachmatiuk, Opt. Expr. **30**, 23678 (2022).
[10] D.-Q. Yang, B. Duan, X. Liu, A.-Q. Wang, X.-G. Li, Y.-F. Ji, Micromachines **11**, 72 (2020).
[11] Y.N. Zhang, Y. Zhao, R.Q. Lv, Sensors Actuators A Phys. **233**, 374 (2015).
[12] P. Lalanne, S. Mias, J.P. Hugonin, Opt. Express **12**, 458 (2004).
[13] C. Sauvan, G. Lecamp, P. Lalanne, J.P. Hugonin Opt. Expr. **13**, 245 (2005).
[14] J.T. Robinson, C. Manolatou, L. Chen, and M. Lipson, Phys. Rev. Lett. **95**, 143901 (2005).
[15] S. Olyaee, M. Seifouri, R. Karami, A Mohebzadeh-Bahabady, Opt. Quantum Electron. **51**, 1 (2019).

